

PACE: Defying the Scaling Hypothesis of Exploration in Iterative Alignment for Mathematical Reasoning

Jun Rao^{1*} Zixiong Yu^{2*} Xuebo Liu¹ Guhan Chen³ Jing Li¹ Jiansheng Wei² Xiaojun Meng² Min Zhang¹

Abstract

Iterative Direct Preference Optimization has emerged as the state-of-the-art paradigm for aligning Large Language Models on reasoning tasks. Standard implementations (DPO-R1) rely on Best-of-N sampling (e.g., $N \geq 8$) to mine golden trajectories from the distribution tail. In this paper, we challenge this scaling hypothesis and reveal a counter-intuitive phenomenon: in mathematical reasoning, aggressive exploration yields diminishing returns and even catastrophic policy collapse. We theoretically demonstrate that scaling N amplifies verifier noise and induces detrimental distribution shifts. To resolve this, we introduce **PACE** (Proximal Alignment via Corrective Exploration), which replaces brute-force mining with a generation-based corrective strategy. Operating with a minimal budget ($2 < N < 3$), PACE synthesizes high-fidelity preference pairs from failed explorations. Empirical evaluations show that PACE outperforms DPO-R1 ($N = 16$) while using only about 1/5 of the compute, demonstrating superior robustness against reward hacking and label noise.

1. Introduction

The alignment of Large Language Models (LLMs) has evolved from static Supervised Fine-Tuning (Rao et al., 2024; Liu et al., 2024a; Wang et al., 2025)(SFT) to dynamic, preference-based (Rao et al., 2025a) reinforcement learning (RL). While algorithms like PPO (Schulman et al., 2017) initially dominated the landscape, recent advances have converged on Iterative Direct Preference Optimization (Iterative DPO) as the state-of-the-art paradigm for reasoning

*Equal contribution ¹Institute of Computing and Intelligence, Harbin Institute of Technology, Shenzhen, China ²Huawei Large Model Data Technology Lab ³Department of Statistics and Data Science, Tsinghua University, Beijing, China. Correspondence to: Xuebo Liu <liuxuebo@hit.edu.cn>, Xiaojun Meng <xiaojun.meng@huawei.com>.

Preprint. February 6, 2026.

tasks (Rafailov et al., 2023; Pang et al., 2024; Yuan et al., 2024; Zhang et al., 2025; Rao et al., 2025b). In this setting, the model acts as its own data generator, iteratively exploring reasoning paths and updating its policy to maximize the likelihood of preferred trajectories over rejected ones.

To construct high-quality preference pairs (y_w, y_l) within this loop, the prevailing industry standard is Best-of-N (BoN) DPO (Dubey et al., 2024; Liu et al., 2024b) (DPO-R1, Zhang et al. 2025). This strategy relies on “brute-force” exploration: for a given prompt, the model generates a large budget of candidate responses (e.g., $N = 16$). A verifier or reward model then acts as a filter, selecting the highest-scoring trajectory as the winner y_w and a lower-scoring one as the loser y_l . The underlying assumption driving this approach is that more exploration yields better positive samples, which in turn drives better alignment. However, we challenge the optimality of this scaling exploration paradigm. We argue that high- N sampling is not merely computationally expensive and introduces fundamental optimization risks. First, Best-of-N (BoN) acts as an adversarial miner against the reward function. As N increases, the probability of selecting false positives, trajectories that exploit verifier noise or spurious correlations, approaches certainty (Gao et al., 2023). Consequently, DPO-R1 often prioritizes lucky guesses over robust reasoning. Second, even with a perfect verifier, constructing y_w from the extreme tail of the generation distribution induces a significant distribution shift. This process forces the model to update towards outlier regions with low probability support, thereby exacerbating optimization instability and excessive KL divergence (Kumar et al., 2020; Lambert & Calandra, 2024).

In this paper, we propose PACE (Proximal Alignment via Corrective Exploration), a data-efficient framework that achieves superior alignment using a minimal sampling budget ($N = 2$). Our core insight is that gradient quality matters more than sample perfection. Unlike DPO-R1, which selects disparate samples from a large pool, PACE synthesizes high-information pairs from failed attempts. When the model generates an incorrect solution under exploration, we rectify the reasoning path via hindsight correction. This process transforms the original error (Hard Negative) and the corrected path (Proximal Positive) into a proximal preference

pair. Because these two trajectories share semantic structure but diverge in logical validity, they provide a sharper, more stable gradient signal than the random DPO-R1 pairs.

Our contributions are as follows:

- We formalize the trade-off between exploration breadth (N) and robustness, proving that high- N sampling in DPO-R1 increases susceptibility to label noise and verifier hacking compared to proximal sampling.
- We introduce PACE, which replaces the selection-based Best-of- N strategy with a generation-based corrective strategy. Compared to DPO-R1 $N=16$, it can achieve $4\sim 5 \times$ the acceleration and ensure similar effectiveness.
- We demonstrate that PACE matches or exceeds the performance of DPO-R1 ($N = 16$) on mathematical reasoning benchmarks. Crucially, in noisy-label experiments, where 20% of ground truths are corrupted, PACE maintains robust performance, whereas DPO-R1 suffers collapse, highlighting the fragility of aggressive rejection sampling.

2. Related Work

Iterative Alignment and the Limits of Best-of-N The alignment of LLMs has rapidly transitioned from online RL (e.g., PPO, Schulman et al. 2017) to offline and iterative paradigms. Direct Preference Optimization (DPO, Rafailov et al. 2023) and its iterative variants, such as SPIN (Chen et al., 2024) and Self-Rewarding LMs (Yuan et al., 2024), have emerged as standard protocols. In these frameworks, the model generates its own training data, creating a self-reinforcing loop. To construct preference pairs (y_w, y_l) within this loop, the dominant strategy is Best-of- N DPO (DPO-R1), which utilizes Rejection Sampling to filter high-quality trajectories from a large pool ($N \geq 16$) (Touvron et al., 2023; Dubey et al., 2024; Nakano et al., 2022). While effective for static datasets, scaling N in an iterative setting presents fundamental risks. Gao et al. (2023) demonstrated that aggressive BoN selection exacerbates Reward Hacking, as the policy overfits to the proxy reward model’s flaws. Furthermore, Lambert & Calandra (2024) identified that selecting from the distribution tail induces a severe distribution shift, pushing the training data outside the model’s trust region and causing optimization instability. Unlike prior works that prioritize exploration breadth (scaling N), we advocate for proximal exploration. By constraining the sampling budget ($N = 2$), PACE mitigates the risk of adversarial mining against the verifier, ensuring that gradient updates remain robust to label noise and distribution shifts.

Self-Correction and Data-Efficient Learning Leveraging a model’s own outputs for improvement is a core theme in recent research. STaR (Self-Taught Reasoner, Zelikman et al. 2022) and RestEM (Singh et al.) adopt a “generate-and-filter” approach, fine-tuning only on correct trajectories.

However, this strategy is sample-inefficient as it ignores the valuable learning signal present in failure cases. Another line of work, such as Self-Refine (Madaan et al., 2023) and Reflexion (Shinn et al., 2023), employs inference-time prompting to correct errors. While effective, these methods incur significant computational overhead during deployment and do not inherently internalize the correction capability into the model weights. For negative learning, techniques like Hindsight Experience Replay (HER, Andrychowicz et al. 2017) in RL and Unlikelihood Training (Welleck et al., 2019) in NLP attempt to learn from failures. We bridge the gap between self-correction and Iterative DPO. SDPO (Hübotter et al., 2026) leverages distillation to integrate feedback from erroneous trajectories, yielding distilled signals that are friendly (Rao et al., 2023; 2026) for subsequent self-distillation of the model. Unlike STaR, which discards errors, PACE treats them as Hard Negatives. Unlike inference-time correction methods, PACE uses a hindsight correction mechanism to synthesize high-quality positive samples from these negatives. This constructs high-information pairs that explicitly teach the model to distinguish between its original error and the corrected logic, achieving superior alignment efficiency.

3. The Risks of Best-of-N

We analyze the learning dynamics of Iterative DPO under the BoN sampling strategy. While scaling inference compute (increasing N) is beneficial for test-time performance, we argue that naively using it for training data generation introduces two fundamental pathologies: False Positive Amplification (susceptibility to reward noise) and Distributional Shift (violating the trust region).

Let $\pi_{\text{ref}}(y|x)$ be the reference policy (i.e., the policy from the previous iteration), and $\mathcal{V}(y, x)$ be a verifier (or reward function) approximating the ground truth $R(y, x)$. In standard DPO-R1, for a prompt x , we sample $\mathcal{Y}_N = \{y_i\}_{i=1}^N \sim \pi_{\text{ref}}(\cdot|x)$ to construct preference pairs (y_w, y_l) via:

$$y_w \in \mathcal{Y}_W = \arg \max_{y \in \mathcal{Y}_N} \mathcal{V}(y, x), \quad y_l \in \mathcal{Y}_N \setminus \mathcal{Y}_W. \quad (1)$$

The policy is then updated to minimize the DPO loss \mathcal{L}_{DPO} .

3.1. False Positive Amplification

In real-world scenarios, the verifier \mathcal{V} is rarely a perfect oracle. It may contain noise (e.g., labeling errors) or structural biases (e.g., reward hacking spots). We demonstrate that increasing N turns the sampling process into an adversarial miner against the verifier. Consider a challenging problem x . We partition the solution space into the true solution set $\mathcal{T} = \{y \mid R(y) = 1\}$ and the hallucinated set $\mathcal{H} = \{y \mid R(y) = 0, \mathcal{V}(y) = 1\}$. The generation process is modeled as follows: the model produces a valid reasoning

path with probability $\alpha = P(y \in \mathcal{T} | x)$. If the reasoning fails, the model may still trigger a verifier flaw with a conditional intrinsic defect rate $\epsilon = P(y \in \mathcal{H} | y \notin \mathcal{T})$. Consequently, the verifier pass probability $\rho = P(\mathcal{V}(y) = 1)$ is $\rho = \alpha + (1 - \alpha)\epsilon$. Since the verifier cannot distinguish between true and spurious solutions, the probability that a selected positive sample is a false positive (FP) is given by:

$$\Psi(\alpha) = P(y \in \mathcal{H} | \mathcal{V}(y) = 1) = \frac{(1-\alpha)\epsilon}{\alpha + (1-\alpha)\epsilon}. \quad (2)$$

From a prior perspective, the FP probability (2) is formally independent of N . However, since DPO training necessitates the construction of positive-negative pairs, increasing N effectively induces a non-random drift in the distribution of training samples: as multiple attempts raise the probability of passing the verifier, it introduces challenging tasks that would rarely yield a correct solution under smaller N . These newly incorporated samples typically exhibit an extremely low empirical pass rate $\hat{\rho}$. For instance, when the sample budget increases from $N - 1$ to N , the marginal observed pass rate for a newly activated sample is merely $1/N$. Based on this observation, we employ Maximum Likelihood Estimation (MLE) to perform a posterior correction on (2). Specifically, the MLE of the model's intrinsic reasoning capability $\hat{\alpha}$ is given by (see Appendix A for details):

$$\hat{\alpha} = \Pi_{[0,1]} \left(\frac{\hat{\rho} - \epsilon}{1 - \epsilon} \right) = \max \left(0, \frac{\hat{\rho} - \epsilon}{1 - \epsilon} \right), \quad (3)$$

where $\Pi_{[0,1]}$ denotes the projection onto the interval $[0, 1]$. Combining the monotonicity of (3) and (2), it follows that the FP probability decreases monotonically with the $\hat{\rho}$. Each time the sample budget increases by 1, the empirical pass rate $\hat{\rho}$ of newly added samples successively decreases ($\sim 1/N$). Consequently, while increasing N expands the scale of the training set, it also systematically introduces marginal samples with a heightened risk of being false positives, thereby exposing the model to significant reward pitfalls. In contrast, PACE's constrained exploration minimizes the “surface area” exposed to verifier noise, yielding a robust training signal even under imperfect supervision.

3.2. Optimization Instability via Distributional Shift

We previously discussed how increasing N introduces more false positive samples. However, even with a perfect validator \mathcal{V} (i.e., $\epsilon = 0$), a large N still causes deviation from the trust region. The core premise of stable RL methods, such as PPO, is to maintain the trust region, ensuring that the target distribution does not excessively diverge from the current policy. We further demonstrate that the BoN method with a large N implicitly violates this principle.

To improve model performance, we define a target distribution $\pi_{\text{new}}(y|x)$ such that the probability of producing the correct answer for a given sample is at least $\eta > \alpha$. During the fine-tuning or alignment process, the objective is

for the trained model distribution to converge toward π_{new} . However, achieving this target distribution inevitably entails a deviation from the reference distribution. If there is a significant gap between the original success probability α and the target probability η , the KL divergence between the two distributions must possess a non-trivial lower bound. According to the Data Processing Inequality, the minimum cost of this distributional shift can be expressed as:

$$\mathbb{D}_{\text{KL}}(\pi_{\text{new}} \| \pi_{\text{ref}}) \geq \eta \log \frac{\eta}{\alpha} + (1 - \eta) \log \frac{1 - \eta}{1 - \alpha}. \quad (4)$$

As previously discussed, the introduction of new samples as N increases typically corresponds to a lower observed pass rate, which tends to result in a lower model accuracy α , thereby leading to greater distributional deviation. Under the assumption of a perfect verifier ($\epsilon = 0$), according to (3), the posterior estimate of the model accuracy is equivalent to the sample pass rate $\hat{\rho}$. For an incremental budget increase from $N - 1$ to N , considering a newly introduced sample (where $\hat{\alpha} = 1/N$), the lower bound (LB) in (4) evolves as:

$$\text{LB Estimation} \sim \eta \log N - H(\eta) + \Omega(1/N), \quad (5)$$

where $H(\eta)$ denotes the binary entropy function. The detailed derivation is provided in Appendix B.

When training on datasets constructed via $N = 16$ (or 64), we force the model to update towards outlier trajectories. This large distribution shift ($\Delta\pi$) often exceeds the stable learning rate capacity of the optimizer, leading to policy collapse or overfitting to specific, narrow reasoning paths, as observed empirically in Gao et al. (2023) and Lambert & Calandra (2024). By constraining $N = 2$, PACE implicitly acts as a regularizer, keeping the target distribution within the proximal trust region of the current policy.

3.3. Information Gain via Hard Negatives

Finally, we consider the quality of the learning signal. The gradient of the DPO loss is scaled by $\sigma(\hat{r}_\theta(y_l) - \hat{r}_\theta(y_w))$, where \hat{r}_θ is the implicit reward. In DPO-R1 ($N = 16$), y_w is the “best” of many, while y_l is often a random “loser”. Standard DPO-R1 constructs Easy Pairs where y_w and y_l are semantically distant, leading to optimization shortcuts. In contrast, PACE constructs Proximal Pairs that lie close to the decision boundary. Theoretically, optimizing against these Hard Negatives maximizes the information gain per update, forcing the model to refine specific reasoning steps rather than memorizing surface-level heuristics.

4. Methods

As shown in Figure 1, we present PACE, a framework designed to maximize alignment efficiency by prioritizing logical density over search breadth. Guided by our theoretical analysis (Section 3), PACE departs from the Select-from-

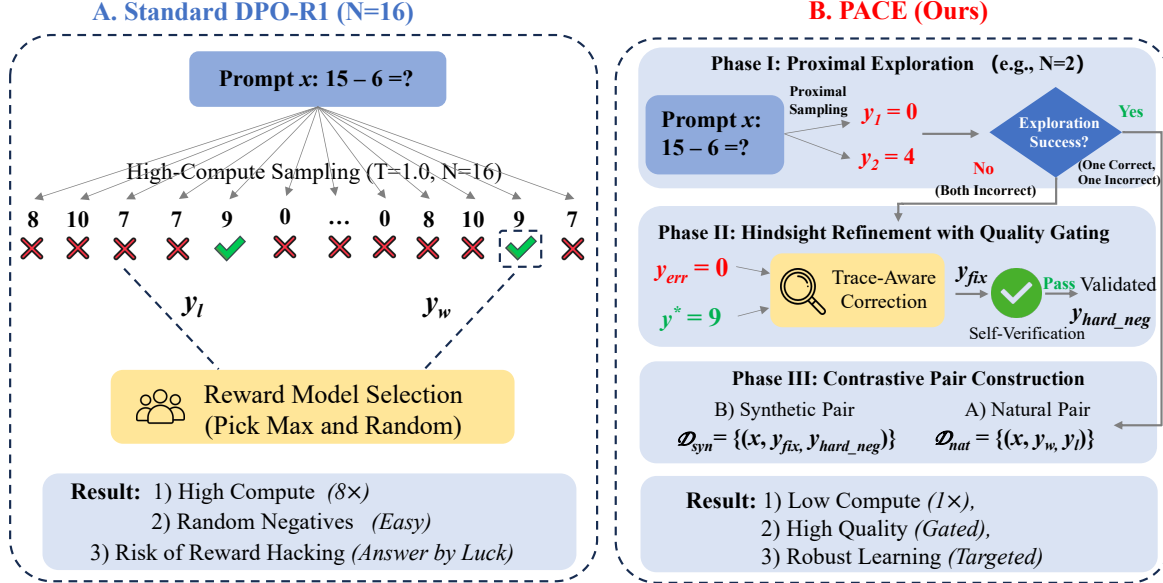


Figure 1. Overview of PACE vs. Standard Best-of-N DPO. (A) Standard BoN ($N = 16$): Relies on high-compute sampling to mine positive signals, risking reward hacking where models match labels through flawed logic. (B) PACE (Ours): A three-phase pipeline: (I) Proximal Exploration ($N = 2$) to minimize compute; (II) Hindsight Refinement with logical gating to synthesize verified corrections (y_{fix}) from failure traces (y_{err}); (III) Contrastive Construction of high-density pairs. PACE achieves superior reasoning alignment with $6 \times$ lower overhead and higher resistance to label noise by prioritizing logical density over search breadth.

Many paradigm of BoN, which relies on high-compute sampling to mine positive signals. Instead, it adopts a Generate-and-Correct paradigm. The overall procedure is summarized in Algorithm 1 in the Appendix.

4.1. Proximal Exploration

To avoid the $\Omega(\log N)$ distribution shift inherent in high- N sampling (Section 3.2), PACE restricts the sampling budget to the minimal sufficient set required to estimate local epistemic uncertainty. For a given prompt x , we generate exactly two trajectories $\mathcal{Y} = \{y_1, y_2\}$ from the current policy π_θ . Generated via stochastic sampling with temperature $T = 1.0$. This probes the local variance of the policy.

Theoretical Justification: This $N = 2$ strategy serves as a Proximal Probe. Unlike $N = 16$, which searches for outliers far from the mean, $N = 2$ assesses whether the mass of the current distribution $\pi_\theta(\cdot | x)$ covers the correct solution. If both samples fail, it indicates a lack of capability (or high uncertainty) within the trust region, signaling the need for correction rather than further random searching.

4.2. Hindsight Refinement with Quality Gating

Trace-Aware Correction. Unlike standard self-correction which relies on generic prompts, we utilize a **Trace-Aware** strategy. We provide the model with its own error trace y_{err} and the ground truth label y^* . The instruction requires the model to identifying the logical divergence between y_{err}

and y^* and generate a corrected path y_{fix} .

$$y_{fix} \sim \pi_\theta(\cdot | x, y_{err}, y^*, \text{instruction}) \quad (6)$$

The Quality Gate (Self-Verification). A known risk of label-conditioned generation is “rationalization”, where the model hallucinates a flawed reasoning chain that coincidentally ends in the target number. To filter these toxic samples, we apply a strict **Consistency Filter**:

1. We strip the final answer from y_{fix} , retaining only the reasoning steps r_{fix} .
2. We verify if the reasoning strictly entails the answer: $\mathbb{I}(\text{Greedy}(x, r_{fix}) == y^*)$.

Trajectories that fail this check are discarded, ensuring only grounded, logically valid corrections enter the training pool.

4.3. Contrastive Pair Construction

The core innovation of PACE lies in how it constructs the preference dataset \mathcal{D} for DPO. We categorize the outcomes of Phase I into two scenarios, each yielding a distinct type of gradient signal. The final y_{fix} has been obtained.

Scenario A: The Natural Pair (Exploration Success) If one sample is correct (y_w) and the other incorrect (y_l) during the initial $N = 2$ rollout, we construct a standard preference pair. If one sample is correct (y_w) and the other incorrect (y_l) during the initial $N = 2$ rollout, we construct a standard preference pair. This captures data within the model’s

current competence, reinforcing known capabilities.

$$\mathcal{D}_{nat} = \{(x, y_w, y_l)\} \quad (7)$$

Scenario B: The Synthetic Pair (Exploration Failure) If both initial samples are incorrect, we utilize the refined trajectory y_{fix} from Phase II. We select the original incorrect sample, denoted as y_{hard_neg} , to serve as the loser.

$$\mathcal{D}_{syn} = \{(x, y_{fix}, y_{hard_neg})\} \quad (8)$$

Why this matters (Gradient Efficiency): In standard BoN, the winner and loser are often semantically distant (a random lucky guess vs. a random failure), leading to high variance updates. In PACE, y_{fix} is a **Proximal Counterfactual** to y_{greedy} , they share the same prompt and potentially similar initial steps, diverging only at the critical error. Optimizing against such **Hard Negatives** provides a high-density gradient signal, effectively suppressing the specific error mode without disrupting the rest of the policy.

Finally, we use \mathcal{L}_{DPO} optimizes the relative log-ratios of the pairs constructed in Phase III:

$$\mathcal{L}_{DPO}(\pi_\theta, \pi_{ref}) = -\mathbb{E}_{(x, y_w, y_l) \sim \mathcal{D}} \left[\log \sigma \left(\beta \log \frac{\pi_\theta(y_w|x)}{\pi_{ref}(y_w|x)} - \beta \log \frac{\pi_\theta(y_l|x)}{\pi_{ref}(y_l|x)} \right) \right]. \quad (9)$$

4.4. Complexity Analysis

Standard Best-of-N strategies suffer from static computational rigidity: the budget is fixed at N regardless of prompt difficulty. In contrast, PACE employs a dynamic allocation strategy, expending additional compute only when epistemic uncertainty is high (i.e., exploration failure). Given that the verification time is relatively negligible, we will disregard this portion of the time in our discussion.

Let C_{gen} be the unit cost of generating one trajectory. The expected computational cost per prompt for PACE is:

$$\mathbb{E}[\mathcal{C}_{PACE}] = (2 + P(\text{fail}|x, \pi_\theta) \cdot K) C_{gen} \quad (10)$$

where $P(\text{fail}|x, \pi_\theta)$ is the probability that the initial proximal exploration ($N = 2$) fails to yield a correct solution, and K is the refinement budget (typically $K = 1$). This formulation yields three critical efficiency properties: 1) **Amortized Efficiency**: For easy instances where $P(\text{fail}) \rightarrow 0$, the cost converges to the lower bound $2C_{gen}$. Standard BoN ($N = 16$) remains statically inefficient at $16C_{gen}$. 2) **Bounded Worst-Case**: Even for hard failures ($P(\text{fail}) \rightarrow 1$), the cost is bounded by $(2 + K)C_{gen}$. With $K = 1$, PACE achieves a $5.3 \times$ speedup over the $N = 16$ baseline in the worst-case scenario. 3) **Self-Optimizing Dynamics**: Crucially, as the policy π_θ improves during DPO training, the failure rate $P(\text{fail})$ naturally diminishes. Consequently, PACE becomes progressively cheaper throughout the training lifecycle, whereas BoN costs remain constant.

5. Experiments

5.1. Setup

Benchmarks: We follow Yang et al. (2024) using common English math benchmarks, Math (Hendrycks et al., 2021b), and using different sets of math tests at different stages to test stronger math skills, such as Minerva Math (Lewkowycz et al., 2022), Gaokao 2023 En (Liao et al., 2024), Olympiad Bench (He et al., 2024), and AMC 23 (AoPS, 2023). We report greedy performance on all benchmarks in the zero-shot setting, except for the Amc23. Considering the limited size of Amc23, we sample 8 times (avg@8) for each question to mitigate randomness. During the answer generation process for these two challenge datasets, we use a temperature of 0.1 and a top-p of 0.95.

Baselines and Models: To rigorously isolate the contribution of our proposed method, we compare PACE against three distinct tiers of baselines: DPO-R1 ($N = 8$ or 16): The current industry standard for iterative alignment (Dubey et al., 2024). For each prompt, we sample $N = 8$ or 16 trajectories at temperature $T = 1.0$. The trajectory maximizing the verifier score is selected as y_w , and a random failing trajectory is selected as y_l . This baseline represents the high-resource upper bound. DPO-R1 ($N = 2, 4$) (The Compute-Matched Baseline): A naive implementation of DPO restricted to the same sampling budget as PACE ($N = 2, 4$). It selects the best of N samples without any corrective mechanism. This baseline is critical for ablation: comparisons against it demonstrate that PACE’s gains stem from the quality of the corrective pairs (Hindsight Refinement). We evaluate our method on three state-of-the-art RL-tuned models (Llama-3.1-8B-Instruct and Qwen3-4B/8B-Instruct), representing the strongest reasoning capabilities under the 8B parameter class. Given that the base models have already been saturated with complex reasoning capabilities through intensive RL (GRPO/PPO), training on extended Think trajectories via DPO is computationally redundant and resource-intensive for tasks that do not require long-form thought. Consequently, we adopt a “No-Think” mode to ensure efficient logical alignment while avoiding the unnecessary overhead of over-optimizing intermediate reasoning tokens on targeted datasets.

5.2. Main Results

We present the evaluation results across five mathematical reasoning benchmarks in Table 1. The results reveal a critical limitation in standard iterative alignment strategies and highlight the efficiency of our proposed method.

Efficiency We compared the average seconds required for each method to process a single sample, with 40,000 samples processed per iteration. In the traditional DPO-R1 baseline, the processing time per sample increases linearly

Table 1. Main Results on Mathematical Reasoning. We evaluate PACE against DPO-R1 baselines across varying sampling budgets (N). We also report the corresponding average number of training samples and the average time (in seconds) required to process a single sample. Note the Efficiency Paradox: While DPO-R1 (High) consumes $16\times$ sampling compute, its sample yield and final performance are often inferior to PACE ($2 < N < 3$), balancing time and effectiveness. This highlights that proximal refinement serves as a more **cost-effective** mechanism for reasoning alignment than brute-force exploration.

METHOD	COMPUTE	TRAINABLE	PROCESSING	STANDARD		EXAM	COMPETITION		AVG.
	COST (\downarrow)	PAIRS	TIME (\downarrow)	MATH500	MINERVA	COLLEGE	OLYMPIAD	AMC23	
<i>Panel A: Llama-3.1-8B-Instruct</i>									
INSTRUCT (BASE)	-	-	-	29.0	16.5	21.3	7.3	15.3	17.9
DPO-R1 (LOW)	$N = 2$	5,246	0.8	37.8	18.8	24.7	9.3	17.8	21.7
DPO-R1 (MIDDLE)	$N = 4$	9,692	1.6	34.8	18.0	23.7	8.9	18.4	20.8
DPO-R1 (ZHANG ET AL., 2025)	$N = 8$	13,224	2.4	35.8	15.8	22.2	8.7	18.8	20.3
DPO-R1 (HIGH)	$N = 16$	16,241	4.0	35.6	19.1	23.0	8.4	19.4	21.1
PACE (OURS)	$2 < N < 3$	6,197	0.8	37.0	21.3	24.9	9.9	20.3	22.7
<i>Panel B: Qwen3-4B-Instruct</i>									
INSTRUCT (BASE)	-	-	-	84.6	34.6	44.9	47.4	64.4	55.2
DPO-R1 (LOW)	$N = 2$	3,479	0.9	84.2	37.1	46.8	50.7	65.6	56.9
DPO-R1 (MIDDLE)	$N = 4$	5,127	1.2	84.2	39.0	47.6	50.4	67.8	57.8
DPO-R1 (ZHANG ET AL., 2025)	$N = 8$	8,403	2.8	84.4	38.6	48.1	48.9	68.8	57.8
DPO-R1 (HIGH)	$N = 16$	8,964	5.2	84.4	40.8	47.6	50.8	66.9	58.1
PACE (OURS)	$2 < N < 3$	10,717	1.0	82.2	39.7	47.4	50.8	69.4	57.9
<i>Panel C: Qwen3-8B-Instruct</i>									
INSTRUCT (BASE)	-	-	-	81.2	33.5	44.6	49.9	63.7	49.6
DPO-R1 (LOW)	$N = 2$	3,403	1.4	83.2	33.5	45.8	49.9	71.9	56.9
DPO-R1 (MIDDLE)	$N = 4$	6,073	2.2	82.4	37.1	46.5	50.5	66.2	56.5
DPO-R1 (ZHANG ET AL., 2025)	$N = 8$	10,211	4.8	83.2	36.0	47.1	50.7	67.5	56.9
DPO-R1 (HIGH)	$N = 16$	10,543	7.2	83.2	36.0	46.7	50.5	67.5	56.8
PACE (OURS)	$2 < N < 3$	9,028	1.7	84.4	39.3	46.8	49.6	71.6	58.3

with the sampling budget N . For example, on the Qwen3-4B model, DPO-R1 (High, $N = 16$) takes up to 5.2 seconds, while PACE completes in just 1.0 seconds, achieving approximately $5.2\times$ acceleration.

Effectiveness Experimental results demonstrate that PACE achieves significantly higher sample utilization efficiency than baseline models while maintaining extremely low computational costs ($2 < N < 3$). Taking Llama-3.1-8B-Instruct as an example, PACE achieved an average score of 22.7 by generating only 6,197 training pairs. This significantly outperforms DPO-R1 (High, $N = 16$), which consumed 16,241 pairs but only achieved 21.1 points. Increasing the sampling budget N grows the dataset size, but it triggers an inverse scaling law where more data actually yields lower performance.

The Luck Trap happens because brute-force sampling at high N selects lucky guesses, solutions with correct answers but broken logic, from the distribution’s tail. In contrast, PACE employs Hindsight Refinement to transform discarded failed attempts into high-quality proximal refinement pairs. On Qwen3-4B, while PACE’s average score (57.9) is nearly on par with DPO-R1 (High)’s 58.1, its core advantage lies in its exceptionally high computational efficiency. PACE requires only a minimal sampling time (1.0) to generate as many as 10,717 high-quality training pairs. In contrast, DPO-R1 (High) incurs a substantial sampling

Table 2. Ablation Study. We isolate the contribution of each PACE component by replacing it with a standard baseline variant.

MODULE	ABLATION VARIANT	ACC. (%)	Δ
PACE (FULL)	TRACE-AWARE + PROXIMAL + VERIFIED	22.7	-
<i>1. Refinement</i>	w/ LABEL-ONLY GUIDANCE (NO TRACE)	18.0	-4.7
	NO REFINEMENT (DPO-R1, $N = 2$)	21.7	-1.0
<i>2. Pairing</i>	w/ RANDOM NEGATIVES	19.8	-2.9
<i>3. Gating</i>	w/o CONSISTENCY FILTER	21.0	-1.7

cost (5.2) of $N = 16$ to generate 8,964 pairs. This shows that PACE achieves performance comparable to high-budget benchmarks with approximately $5\times$ acceleration, maintaining a significant advantage in output efficiency per sample and the use of computational resources.

5.3. Ablation Studies

To dissect the contribution of each component in PACE, we conducted an ablation study on the Llama-3-8B model (Table 2). The results reveal that Trace-Aware Refinement is the most critical factor; replacing it with Label-Only guidance leads to the most significant performance degradation (-4.7%). This confirms that conditioning on the specific error trace is essential to force comparative debugging and prevent the model from merely rationalizing the target label. Furthermore, substituting Proximal Pairs with random negatives results in a -2.9% drop, validating our hypothesis that

Table 3. Iterative Performance and Noise Robustness Analysis on Llama-3.1-8B (20% Label Noise). The left panel shows accuracy evolution across 4 iterations. The right panel provides a diagnostic snapshot of the training buffer: **Yield** refers to the number of training pairs, and **Noise Hit Rate (NHR)** measures the percentage of samples where the model successfully mined a trajectory matching the corrupted "0" label. PACE achieves superior stability by maintaining high signal purity.

Method	Accuracy (Iter 1-4) ↑				Noise Diagnostics (Snapshots)			
	It. 1	It. 2	It. 3	It. 4	Yield (Clean)	Yield (Noisy)	Drop %	NHR ↓
DPO-R1 ($N = 2$) (Baseline)	20.0	19.1	16.8	12.7	4,221	3,722	11.8%	4.3%
DPO-R1 ($N = 16$) (Scaling)	19.5	20.3	20.8	19.1	15,719	14,823	5.7%	28.1%
PACE (Ours)	18.3	19.1	20.1	20.4	6,159	5,317	13.7%	4.9%

optimization against hard, on-policy negatives yields higher-fidelity gradient signals than random baselines. Finally, removing the Consistency Filter causes a **-1.7%** decline, underscoring the necessity of quality gating to prevent hallucinated reasoning from polluting the training dynamics.

6. Analysis

6.1. Resilience to Label Noise

Standard rejection sampling strategies implicitly assume a high-fidelity verifier. However, in real-world scenarios, reward signals are often noisy or exploitable. To empirically validate our theoretical hypothesis (Section 3.1), we conduct a stress test designed to induce Reward Hacking. To further investigate the resilience of PACE, we track the iterative alignment of Llama-3.1-8B under 20% label noise (Table 3, e.g., changing the ground truth to 0), a setting we term the Small-Digit Trap. We report the average results of the dataset in the main table. Our analysis reveals a fundamental divergence in how methods handle corrupted feedback.

While $N = 16$ maintains a higher absolute accuracy in later iterations, its training buffer is heavily compromised by a 28.1% Noise Hit Rate (NHR). However, with the final iteration, the effectiveness declined sharply. This suggests that high- N exploration acts as an *adversarial miner*, effectively synthesizing hallucinations to match erroneous '0' labels. Although the sheer volume of correct samples initially buffers this toxicity, the high NHR poses a risk of long-term policy degradation. Conversely, $N = 2$ exhibits low NHR (4.3%) but suffers from severe signal starvation (Yield Drop 11.8%), causing it to stall at 12.7% accuracy.

PACE resolves this trade-off by achieving a low NHR (4.9%) comparable to $N = 2$, while recovering 42.8% more valid signals through hindsight refinement. The 13.7% yield drop in PACE is a deliberate logical purge, the consistency filter rejects synthesized paths that cannot be logically reconciled with the erroneous labels. This results in the highest iterative performance, proving that **synthesized purity** is a more robust scaling axis than **mined volume** for alignment.

Table 4. Out-of-Domain Generalization. While high- N exploration often leads to alignment tax on OOD tasks, PACE maintains distributional integrity through proximal refinement.

Method	BBH	Code	MMLU	TruthfulQA	Avg.
Llama3.1-8B	56.2	51.7	68.6	37.7	53.5
BoN (2)	58.1	53.9	68.4	38.8	54.8
BoN (8)	57.0 (↓)	52.7 (↓)	68.4 (−)	37.9 (↓)	54.0
Ours	59.1 (↑)	55.3 (↑)	68.3 (↓)	38.2 (↑)	55.2

6.2. Optimization Instability

Generalization We conducted a series of out-of-domain (OOD) benchmarks on the Llama-3.1-8B model, including symbolic reasoning (BBH, Suzgun et al. 2023), programming (HumanEval, Chen et al. 2021, pass@1), general knowledge (MMLU, Hendrycks et al. 2021a), and factuality (TruthfulQA, Lin et al. 2022, MC1). As shown in Table 4, traditional sampling strategies exhibit significant performance degradation across multiple OOD dimensions when increasing the sampling budget N (from 2 to 8), a classic manifestation of adversarial mining causing models to overfit to validator rewards and thereby compromise general capabilities. In contrast, PACE leverages its Proximal Refinement mechanism to substantially enhance mathematical reasoning capabilities while nearly perfectly preserving the model's original distribution. Its average OOD score (55.2) not only significantly outperforms the computationally more expensive BoN (8) baseline (54.0), but also demonstrates positive transfer learning on programming tasks (1.4% improvement over BoN(2)). This demonstrates that PACE achieves efficient logical alignment without sacrificing foundational model intelligence, providing a robust scientific paradigm for resolving the performance-generalization paradox in iterative alignment.

Iterative Dynamics Figure 2 reveals a Quality-Quantity Trade-off in iterative alignment. The DPO-R1 with high sampling budget ($N = 16$) exhibits a classic overfitting trajectory: it starts with strong performance (21.7% in Iter 1) by maximizing coverage of the solution space. However, this advantage is transient; accuracy degrades to 21.1% by Iteration 4. We attribute this collapse to the unsupervised na-

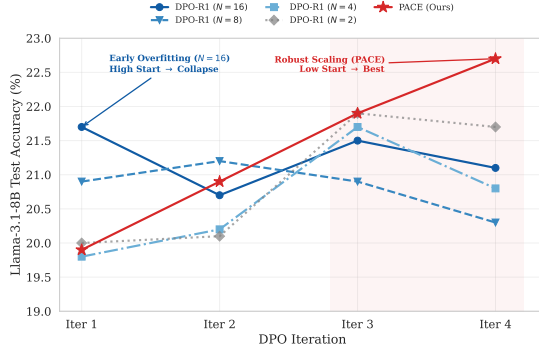


Figure 2. The Dynamics of Iterative Alignment on Llama-3.1-8B.

Table 5. Iso-Data Efficiency Analysis on Llama-3.1-8B. All methods are trained on a fixed budget of **5,000 preference pairs** to isolate the impact of the exploration budget (N) on sample quality. PACE ($N = 2$) achieves superior performance by optimizing information density rather than expanding the search breadth.

Method	Exploration (N)	Accuracy (%)
Standard BoN	2	21.7
Standard BoN	4	22.2
Standard BoN	8	22.3
Standard BoN	16	22.0 ($\uparrow 0.3$)
PACE (Ours)	2	22.5 ($\uparrow 0.8$)

ture of rejection sampling, as the model improves, $N = 16$ retrieves an increasing number of spurious positives (hallucinated reasoning with correct answers) from the distribution tail, which poison the reward signal. In contrast, PACE (red line) demonstrates a robust scaling law. Although it begins with lower accuracy (19.9%), a direct result of our Consistency Filter rejecting low-confidence lucky guesses, it is the only method that maintains monotonic improvement, reaching 22.7% in Iteration 4. This confirms that for iterative learning, the purity of the training signal (ensured by refinement and filtering) is a more critical determinant of long-term performance than the sheer volume of exploration.

6.3. Data Efficiency & Topology

Iso-Data Analysis To further disentangle the impact of data quantity from data quality, we conduct a controlled Iso-Data Analysis on Llama-3.1-8B. In this setting, we strictly fix the training budget to 5,000 preference pairs for all methods, regardless of their exploration budget N .

As shown in Table 5, standard BoN methods exhibit a non-linear relationship between exploration breadth and performance. While increasing N from 2 to 4 yields an initial gain, further scaling to $N = 16$ results in a performance regression. This empirical supports our hypothesis regarding adversarial mining: in the absence of additional logic

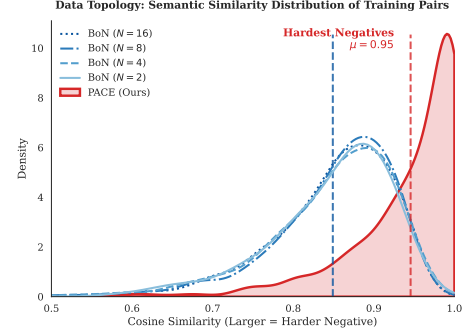


Figure 3. Data Topology Analysis: Hard vs. Easy Negatives.

preserving constraints, a larger search pool ($N = 16$) increases the likelihood of capturing deceptive trajectories, samples that reach the correct ground truth through flawed or accidental reasoning. When these trajectories are used as positive signals in DPO, they introduce gradient noise that misaligns the model’s logical reasoning with its final answers. In stark contrast, PACE ($N = 2$) achieves a peak accuracy of 22.5%, outperforming the $N = 2$ baseline by 0.8% and even surpassing the strongest BoN variant ($N = 4/8$) by 0.5% within the same 5,000-pair budget with fewer exploration attempts. This result provides definitive evidence that the quality of construction (Synthesis) is more vital than the breadth of exploration (Mining).

Semantic Similarity Distribution Instead of analyzing gradients directly (which is noisy), we analyze the geometric relationship between the winner and loser responses. If y_w and y_l are very similar (high cosine similarity), the model cannot rely on length, style, or lexical overlap to distinguish them. It must understand the underlying logic. This implies high gradient efficiency. We investigated the semantic properties of the training pairs constructed by PACE versus DPO-R1 ($N = 16$). We randomly sampled 1,000 pairs from each dataset (PACE refinement and BoN) and computed the Cosine Similarity between the embeddings of the winner (y_w) and loser (y_l) trajectories using a pre-trained sentence encoder. As illustrated in Figure 3, the distribution of PACE pairs (red) is heavily skewed towards high similarity ($\mu \approx 0.95$), whereas DPO-R1 pairs (blue) are distributed across a lower, broader range ($\mu \approx 0.85$). This confirms that PACE synthesizes Proximal Pairs (Hard Negatives). In DPO-R1, the “loser” is often a random failure, semantically distinct from the winner, allowing the model to easily distinguish them via surface-level features (e.g., length or lexical mismatch). This leads to easy wins during optimization and low information gain.

In contrast, PACE’s corrective pairs share the same reasoning skeleton and diverge only at the specific error step. Discriminating between these fine-grained differences forces

the model to perform deep reasoning alignment, explaining PACE’s superior efficiency per training step.

7. Conclusion

In this work, we revisited the widely held assumption that scaling inference compute during data generation is the only path to better alignment. Through both theoretical analysis and empirical rigor, we identified the hidden costs of Best-of-N DPO: its tendency to violate trust regions via distribution shift and its susceptibility to amplifying label noise. We proposed PACE, a novel alignment framework that prioritizes gradient quality over sample perfection. By constraining exploration to the proximal region and employing Label-Conditioned Correction, PACE transforms the model’s own errors into high-fidelity “Hard Negative” training signals. Our experiments demonstrate that PACE not only matches the state-of-the-art performance of computationally expensive baselines but does so with significantly greater efficiency and robustness.

Impact Statement

As LLM post-training scales, the computational cost of data generation becomes a bottleneck. PACE offers a sustainable path forward, demonstrating that smarter data synthesis can replace larger data mining. This has significant implications for democratizing the training of reasoning models, particularly in domains where verified data is scarce or verifiers are imperfect. While our current work focuses on mathematical reasoning with ground-truth labels, future directions include extending the corrective mechanism to open-ended generation tasks using AI-based feedback (e.g., LLM-as-a-Judge).

References

Andrychowicz, M., Wolski, F., Ray, A., Schneider, J., Fong, R., Welinder, P., McGrew, B., Tobin, J., Pieter Abbeel, O., and Zaremba, W. Hindsight experience replay. *Advances in neural information processing systems*, 30, 2017. URL <https://papers.nips.cc/paper/7090-hindsight-experience-replay>.

AoPS. AMC Problems and Solutions, 2023. URL <https://huggingface.co/datasets/AI-MO/aimo-validation-amc>.

Chen, M., Tworek, J., Jun, H., Yuan, Q., de Oliveira Pinto, H. P., Kaplan, J., Edwards, H., Burda, Y., Joseph, N., Brockman, G., et al. Evaluating large language models trained on code, 2021. URL <https://arxiv.org/abs/2107.03374>.

Chen, Z., Deng, Y., Yuan, H., Ji, K., and Gu, Q. Self-play fine-tuning converts weak language models to strong language models. In *Forty-first International Conference on Machine Learning, ICML 2024, Vienna, Austria, July 21-27, 2024*. OpenReview.net, 2024. URL <https://openreview.net/forum?id=O4cHTxW9BS>.

Dubey, A., Jauhri, A., Pandey, A., Kadian, A., Al-Dahle, A., Letman, A., Mathur, A., Schelten, A., Yang, A., Fan, A., et al. The llama 3 herd of models. *arXiv preprint arXiv:2407.21783*, 2024. URL <https://arxiv.org/abs/2407.21783>.

Gao, L., Schulman, J., and Hilton, J. Scaling laws for reward model overoptimization. In *Proceedings of the 40th International Conference on Machine Learning*, volume 202 of *Proceedings of Machine Learning Research*, pp. 10835–10866. PMLR, 23–29 Jul 2023. URL <https://proceedings.mlr.press/v202/gao23h.html>.

He, C., Luo, R., Bai, Y., Hu, S., Thai, Z., Shen, J., Hu, J., Han, X., Huang, Y., Zhang, Y., Liu, J., Qi, L., Liu, Z., and Sun, M. OlympiadBench: A challenging benchmark for promoting AGI with olympiad-level bilingual multimodal scientific problems. In *Proceedings of the 62nd Annual Meeting of the Association for Computational Linguistics (Volume 1: Long Papers)*, pp. 3828–3850, Bangkok, Thailand, August 2024. Association for Computational Linguistics. URL <https://aclanthology.org/2024.acl-long.211/>.

Hendrycks, D., Burns, C., Basart, S., Zou, A., Mazeika, M., Song, D., and Steinhardt, J. Measuring massive multitask language understanding. In *9th International Conference on Learning Representations, ICLR 2021, Virtual Event, Austria, May 3-7, 2021*. OpenReview.net, 2021a. URL <https://openreview.net/forum?id=d7KBjmI3GmQ>.

Hendrycks, D., Burns, C., Kadavath, S., Arora, A., Basart, S., Tang, E., Song, D., and Steinhardt, J. Measuring mathematical problem solving with the MATH dataset. In *Proceedings of the Neural Information Processing Systems Track on Datasets and Benchmarks 1, NeurIPS Datasets and Benchmarks 2021, December 2021, virtual*, 2021b. URL <https://openreview.net/forum?id=7Bywt2mQsCe>.

Hübotter, J., Lübeck, F., Behric, L., Baumann, A., Bagatella, M., Marta, D., Hakimi, I., Shenfeld, I., Buening, T. K., Guestrin, C., and Krause, A. Reinforcement learning via self-distillation, 2026. URL <https://arxiv.org/abs/2601.20802>.

Kingma, D. P. and Ba, J. Adam: A method for stochastic optimization. In Bengio, Y. and LeCun, Y. (eds.), *3rd International Conference on Learning Representations, ICLR 2015, San Diego, CA, USA, May 7-9*,

2015, Conference Track Proceedings, 2015. URL <https://arxiv.org/abs/1412.6980>.

Kumar, A., Zhou, A., Tucker, G., and Levine, S. Conservative q-learning for offline reinforcement learning. In *Advances in Neural Information Processing Systems*, volume 33, pp. 1179–1191. Curran Associates, Inc., 2020. URL <https://arxiv.org/abs/2006.04779>.

Lambert, N. and Calandra, R. The alignment ceiling: Objective mismatch in reinforcement learning from human feedback, 2024. URL <https://arxiv.org/abs/2311.00168>.

Lewkowycz, A., Andreassen, A., Dohan, D., Dyer, E., Michalewski, H., Ramasesh, V., Slone, A., Anil, C., Schlag, I., Gutman-Solo, T., Wu, Y., Neyshabur, B., Gur-Ari, G., and Misra, V. Solving quantitative reasoning problems with language models, 2022. URL <https://arxiv.org/abs/2206.14858>.

Liao, M., Li, C., Luo, W., Jing, W., and Fan, K. MARIO: MAth reasoning with code interpreter output - a reproducible pipeline. In *Findings of the Association for Computational Linguistics: ACL 2024*, pp. 905–924, Bangkok, Thailand, August 2024. Association for Computational Linguistics. URL <https://aclanthology.org/2024.findings-acl.53/>.

Lin, S., Hilton, J., and Evans, O. TruthfulQA: Measuring how models mimic human falsehoods. In *Proceedings of the 60th Annual Meeting of the Association for Computational Linguistics (Volume 1: Long Papers)*, pp. 3214–3252, Dublin, Ireland, 2022. Association for Computational Linguistics. URL <https://aclanthology.org/2022.acl-long.229/>.

Liu, L., Liu, X., Wong, D. F., Li, D., Wang, Z., Hu, B., and Zhang, M. SelectIT: Selective instruction tuning for LLMs via uncertainty-aware self-reflection. In *The Thirty-eighth Annual Conference on Neural Information Processing Systems*, 2024a. URL <https://openreview.net/forum?id=QNieOPT4fg>.

Liu, T., Zhao, Y., Joshi, R., Khalman, M., Saleh, M., Liu, P. J., and Liu, J. Statistical rejection sampling improves preference optimization. In *The Twelfth International Conference on Learning Representations*, 2024b. URL <https://openreview.net/forum?id=xbjSwrrQOe>.

Madaan, A., Tandon, N., Gupta, P., Hallinan, S., Gao, L., Wiegreffe, S., Alon, U., Dziri, N., Prabhumoye, S., Yang, Y., Gupta, S., Majumder, B. P., Hermann, K., Welleck, S., Yazdanbakhsh, A., and Clark, P. Self-refine: Iterative refinement with self-feedback. In *Thirty-seventh Conference on Neural Information Processing Systems*, 2023. URL <https://openreview.net/forum?id=S37hOerQLB>.

Nakano, R., Hilton, J., Balaji, S., Wu, J., Ouyang, L., Kim, C., Hesse, C., Jain, S., Kosaraju, V., Saunders, W., Jiang, X., Cobbe, K., Eloundou, T., Krueger, G., Button, K., Knight, M., Chess, B., and Schulman, J. Webgpt: Browser-assisted question-answering with human feedback, 2022. URL <https://arxiv.org/abs/2112.09332>.

Pang, R. Y., Yuan, W., Cho, K., He, H., Sukhbaatar, S., and Weston, J. Iterative reasoning preference optimization, 2024. URL <https://arxiv.org/abs/2404.19733>.

Rafailov, R., Sharma, A., Mitchell, E., Manning, C. D., Ermon, S., and Finn, C. Direct preference optimization: Your language model is secretly a reward model. In Oh, A., Naumann, T., Globerson, A., Saenko, K., Hardt, M., and Levine, S. (eds.), *Advances in Neural Information Processing Systems 36: Annual Conference on Neural Information Processing Systems 2023, NeurIPS 2023, New Orleans, LA, USA, December 10 - 16, 2023*, 2023. URL <https://openreview.net/forum?id=HPuSIXJaa9>.

Rao, J., Meng, X., Ding, L., Qi, S., Liu, X., Zhang, M., and Tao, D. Parameter-efficient and student-friendly knowledge distillation. *IEEE Trans. Multim.*, pp. 1–12, 2023. doi: 10.1109/TMM.2023.3321480. URL <https://ieeexplore.ieee.org/document/10272648/>.

Rao, J., Liu, X., Lian, L., Cheng, S., Liao, Y., and Zhang, M. CommonIT: Commonality-aware instruction tuning for large language models via data partitions. In Al-Onaizan, Y., Bansal, M., and Chen, Y.-N. (eds.), *EMNLP*, pp. 10064–10083, Miami, Florida, USA, 2024. Association for Computational Linguistics. doi: 10.18653/v1/2024.emnlp-main.561. URL [https://aclanthology.org/2024.emnlp-main.561/](https://aclanthology.org/2024.emnlp-main.561).

Rao, J., Lin, Z., Liu, X., Ke, X., Lian, L., Jin, D., Cheng, S., Yu, J., and Zhang, M. APT: Improving specialist LLM performance with weakness case acquisition and iterative preference training. In *Findings of the Association for Computational Linguistics: ACL 2025*, pp. 20958–20980, Vienna, Austria, July 2025a. Association for Computational Linguistics. ISBN 979-8-89176-256-5. doi: 10.18653/v1/2025.findings-acl.1079. URL <https://aclanthology.org/2025.findings-acl.1079/>.

Rao, J., Liu, X., Deng, H., Lin, Z., Yu, Z., Wei, J., Meng, X., and Zhang, M. Dynamic sampling that adapts: Iterative

dpo for self-aware mathematical reasoning, 2025b. URL <https://arxiv.org/abs/2505.16176>.

Rao, J., Liu, X., Lin, Z., Ding, L., Li, J., Tao, D., and Zhang, M. Exploring and enhancing the transfer of distribution in knowledge distillation for autoregressive language models. *Knowledge-Based Systems*, 2026. URL <https://www.sciencedirect.com/science/article/abs/pii/S095050705126001255>.

Schulman, J., Wolski, F., Dhariwal, P., Radford, A., and Klimov, O. Proximal policy optimization algorithms. *arXiv preprint arXiv:1707.06347*, 2017. URL <https://arxiv.org/abs/1707.06347>.

Shinn, N., Cassano, F., Gopinath, A., Narasimhan, K. R., and Yao, S. Reflexion: language agents with verbal reinforcement learning. In *Thirty-seventh Conference on Neural Information Processing Systems*, 2023. URL <https://openreview.net/forum?id=vAE1hFcKW6>.

Singh, A., Co-Reyes, J. D., Agarwal, R., Anand, A., Patil, P., Garcia, X., Liu, P. J., Harrison, J., Lee, J., Xu, K., et al. Beyond human data: Scaling self-training for problem-solving with language models. *Transactions on Machine Learning Research*. URL <https://openreview.net/forum?id=1NAyUngGFK>.

Suzgun, M., Scales, N., Schärli, N., Gehrman, S., Tay, Y., Chung, H. W., Chowdhery, A., Le, Q., Chi, E., Zhou, D., et al. Challenging BIG-bench tasks and whether chain-of-thought can solve them. In Rogers, A., Boyd-Graber, J., and Okazaki, N. (eds.), *Findings of the Association for Computational Linguistics: ACL 2023*, pp. 13003–13051, Toronto, Canada, 2023. Association for Computational Linguistics. doi: 10.18653/v1/2023.findings-acl.824. URL <https://aclanthology.org/2023.findings-acl.824/>.

Touvron, H., Lavril, T., Izacard, G., Martinet, X., Lachaux, M., Lacroix, T., Rozière, B., Goyal, N., Hambro, E., Azhar, F., et al. Llama: Open and efficient foundation language models. *arXiv preprint arXiv:2302.13971*, 2023. URL <https://arxiv.org/abs/2302.13971>.

Wang, Z., Wang, Y., Liu, X., Ding, L., Zhang, M., Liu, J., and Zhang, M. AgentDropout: Dynamic agent elimination for token-efficient and high-performance LLM-based multi-agent collaboration. In Che, W., Nabende, J., Shutova, E., and Pilehvar, M. T. (eds.), *Proceedings of the 63rd Annual Meeting of the Association for Computational Linguistics (Volume 1: Long Papers)*, pp. 24013–24035, Vienna, Austria, July 2025. Association for Computational Linguistics. ISBN 979-8-89176-251-0. doi: 10.18653/v1/2025.acl-long.1170. URL <https://aclanthology.org/2025.acl-long.1170/>.

Welleck, S., Kulikov, I., Roller, S., Dinan, E., Cho, K., and Weston, J. Neural text generation with unlikelihood training, 2019. URL <https://arxiv.org/abs/1908.04319>.

Yang, A., Zhang, B., Hui, B., Gao, B., Yu, B., Li, C., Liu, D., Tu, J., Zhou, J., Lin, J., Lu, K., Xue, M., Lin, R., Liu, T., Ren, X., and Zhang, Z. Qwen2.5-math technical report: Toward mathematical expert model via self-improvement, 2024. URL <https://arxiv.org/abs/2409.12122>.

Yuan, W., Pang, R. Y., Cho, K., Li, X., Sukhbaatar, S., Xu, J., and Weston, J. E. Self-rewarding language models. In *Forty-first International Conference on Machine Learning*, 2024. URL <https://arxiv.org/abs/2401.10020>.

Zelikman, E., Wu, Y., Mu, J., and Goodman, N. Star: Bootstrapping reasoning with reasoning. *Advances in Neural Information Processing Systems*, 35:15476–15488, 2022. URL <https://arxiv.org/abs/2203.14465>.

Zhang, H., Yao, J., Ye, C., Xiong, W., and Zhang, T. Online-dpo-r1: Unlocking effective reasoning without the ppo overhead. *Notion Blog*, 2025. URL <https://github.com/RLHFlow/Online-DPO-R1>.

A. Detailed Derivation of False Positive Amplification

This appendix provides a formal derivation to demonstrate that, under conditions of verifier inaccuracy, increasing the sampling budget N leads to a higher FP rate in newly added training samples. This section serves as a supplement and extension to the theoretical analysis in Section 3.1. To maintain the self-sufficiency and completeness of the derivation, some necessary background information is retained, which may partially overlap with the main text.

A.1. Problem Formulation

Consider a (typically challenging) problem x . Let y be a candidate solution generated by the model. Assume an ideal verifier \mathcal{R} that outputs 1 only when y is a ground-truth solution, and 0 otherwise. In practice, however, we employ a verifier \mathcal{V} to approximate the ground truth, which has a certain probability of incorrectly accepting erroneous solutions as correct.

Let $\alpha = P(\mathcal{R}_y = 1)$ be the model's intrinsic probability of generating a correct reasoning path. Let $\epsilon = P(\mathcal{V}_y = 1 | \mathcal{R}_y = 0)$ be the conditional defect rate (noise floor) of the verifier. Assuming the verifier has perfect recall for correct answers, i.e., $P(\mathcal{V}_y = 1 | \mathcal{R}_y = 1) = 1$, the total pass rate ρ by the verifier is:

$$\begin{aligned}\rho &= P(\mathcal{V}_y = 1) = P(\mathcal{V}_y = 1 | \mathcal{R}_y = 1)P(\mathcal{R}_y = 1) + P(\mathcal{V}_y = 1 | \mathcal{R}_y = 0)P(\mathcal{R}_y = 0) \\ &= \alpha + (1 - \alpha)\epsilon = (1 - \epsilon)\alpha + \epsilon \in [0, 1].\end{aligned}\quad (11)$$

Notably, to simplify the analysis and extract core trends, we assume ϵ to be a constant independent of specific instances, representing the verifier's intrinsic defect rate. To be sure, in real-world scenarios, the misjudgment probability of a verifier is influenced by various factors such as problem difficulty or answer-space complexity, just as the random pass rate for multiple-choice questions is typically higher than that for open-ended ones. However, the present theoretical analysis aims to marginalize these individual variances to focus on the evolutionary impact of the sampling budget N on the distribution of valid samples within an idealized and controlled environment. This assumption is analogous to a student adopting a uniform random guessing strategy for all questions that fall beyond their knowledge base.

Furthermore, we define the defect rate as a conditional probability given an incorrect solution, rather than a global probability, to ensure logical self-consistency. This formulation effectively avoids the physically implausible scenario where the total pass rate exceeds 1 when the model's accuracy α is high (the overall pass rate would then become $\alpha + \epsilon$ in this case). Overall, the current assumptions balance modeling simplicity with mathematical rigor.

A.2. False Positive Probability

The probability that a sample is a false positive given it passed the verifier is denoted by $\Psi(\alpha)$. By Bayes' Theorem:

$$\Psi(\alpha) = P(\mathcal{R}_y = 0 | \mathcal{V}_y = 1) = \frac{P(\mathcal{V}_y = 1 | \mathcal{R}_y = 0)P(\mathcal{R}_y = 0)}{P(\mathcal{V}_y = 1)} = \frac{(1 - \alpha)\epsilon}{\alpha + (1 - \alpha)\epsilon}. \quad (12)$$

Taking the derivative with respect to α :

$$\frac{d\Psi}{d\alpha} = \frac{-\epsilon}{(\alpha + (1 - \alpha)\epsilon)^2} < 0. \quad (13)$$

This confirms that $\Psi(\alpha)$ is monotonically decreasing with α . Lower intrinsic reasoning capability α leads to a higher risk of verifier hacking.

A.3. The Impact of Large Sampling Budget on Training Samples

As mentioned earlier, from a prior probability perspective, the theoretical form of FP probability $\Psi(\alpha)$ is determined solely by the model's inherent capability α and the verifier's conditional defect rate ϵ ; it does not depend formally on the sample budget N . However, in the practical implementation of constructing DPO positive-negative sample pairs, the sample distribution undergoes significant shifts due to the selection mechanism.

For highly challenging problems (i.e., samples with a small α), the single-generation pass rate ρ is extremely low. As N increases, the model's "trial space" expands substantially. According to the probability formula

$$\rho_N = 1 - (1 - \rho)^N, \quad (14)$$

the absolute probability that such a sample yields at least one “verified-passing” solution (regardless of its true correctness) and is therefore retained as a positive sample rises accordingly. This implies that large-scale sampling effectively acts as a “probability amplifier,” allowing solutions that would have been filtered out under a small N because of their very low empirical pass rate to gain a higher survival probability in the final training dataset. This “statistical bias” introduced by deeper sampling necessitates a posterior adjustment to the theoretical formula.

It should be noted that we only apply posterior correction to α . This is because in DPO training, we have empirical observations of the pass rate, enabling estimation of α ; however, for ϵ , we lack direct observational data, and therefore it is still assumed to be fixed here.

A.4. MLE of the Intrinsic Capability of Model

For the sake of analytical simplicity, the main text employs MLE for posterior correction. We replicate this approach here to maintain consistency. From (11), we have the relation $\rho = \alpha(1 - \epsilon) + \epsilon$. The MLE for the observed pass rate is $\hat{\rho}$. Substituting this into the relation:

$$\hat{\rho} = \hat{\alpha}(1 - \epsilon) + \epsilon \implies \hat{\alpha} = \frac{\hat{\rho} - \epsilon}{1 - \epsilon}. \quad (15)$$

Accounting for the boundary constraint $\alpha \in [0, 1]$, the projected MLE is:

$$\hat{\alpha} = \Pi_{[0,1]} \left(\frac{\hat{\rho} - \epsilon}{1 - \epsilon} \right) = \max \left(0, \frac{\hat{\rho} - \epsilon}{1 - \epsilon} \right). \quad (16)$$

Combining the monotonicity of (12) and (16), it follows that the FP probability decreases monotonically with the $\hat{\rho}$.

A.5. the Cost of Deep Sampling and Asymptotic Behavior

As mentioned earlier, when N increases, newly added samples typically exhibit a lower empirical pass rate $\hat{\rho}$. Given the monotonic decreasing relationship between the false positive rate and $\hat{\rho}$, this implies that the false positive rate of the newly added samples will correspondingly rise.

Specifically, consider “marginal tasks” where a verified solution emerges for the first time only as the sampling budget increases from $N - 1$ to N . For such tasks, the empirical pass rate $\hat{\rho} = 1/N$ decreases monotonically with N . This indicates a clear trend of marginal quality degradation: as the sampling budget expands, the empirical pass rate of newly incorporated samples continues to decline, leading to a corresponding escalation in the risk of false positives.

Furthermore, as $N \rightarrow \infty$, we observe:

$$\lim_{N \rightarrow \infty} \hat{\alpha} = \max \left(0, \frac{\frac{1}{N} - \epsilon}{1 - \epsilon} \right) = 0, \quad \text{for any } \epsilon > 0. \quad (17)$$

Substituting this into (12), the FP probability for these newly recovered samples approaches:

$$\lim_{\hat{\alpha} \rightarrow 0} \Psi(\hat{\alpha}) = \frac{(1 - 0)\epsilon}{0 + (1 - 0)\epsilon} = 1. \quad (18)$$

This derivation formally captures the False Positive Amplification effect: while increasing N recovers more training data from challenging problems, the marginal gain consists almost entirely of spurious solutions. In the context of DPO, treating these high-FP samples as positive reinforcements directs the model to optimize for verifier loopholes rather than genuine reasoning capabilities.

A.6. Bayesian Posterior Distribution

While the MLE approach provides a straightforward point estimation, it ignores the inherent uncertainty in α given small sample sizes. A more rigorous treatment considers α as a random variable. We assume a non-informative prior $\alpha \sim \mathcal{U}[0, 1]$ (i.e., a uniform distribution, equivalent to Beta(1, 1)). Given the observation $D = \{k, N\}$ (where k represents the observed empirical pass rate of the verifier), the posterior probability density function (PDF) of the latent capability α is proportional to the likelihood $L(\alpha | D)$:

$$L(\alpha | D) \propto [\rho(\alpha)]^k [1 - \rho(\alpha)]^{N-k}, \quad p(\alpha | D) = \frac{[\rho(\alpha)]^k [1 - \rho(\alpha)]^{N-k}}{\int_0^1 [\rho(\alpha)]^k [1 - \rho(\alpha)]^{N-k} d\alpha}. \quad (19)$$

Building on this, we calculate the expectation of the false positive rate under this posterior distribution:

$$\bar{\Psi}(D) = \mathbb{E}_{\alpha|D}[\Psi(\alpha)] = \int_0^1 \Psi(\alpha) p(\alpha | D) d\alpha. \quad (20)$$

As before, we continue to focus on the false positive rate of the additional samples when the sampling budget increases by one, and arrive at the following analogous conclusion:

Proposition A.1 (Monotonicity of Marginal False Positives). *Consider a marginal task where a verified solution is obtained for the first time only at the N -th attempt (i.e., $D_N = \{1, N\}$). The expected false positive (FP) rate of such a sample, denoted by $\bar{\Psi}(N) = \mathbb{E}_{\alpha|D_N}[\Psi(\alpha)]$, is strictly monotonically increasing with respect to the sampling budget N . That is:*

$$N_1 > N_2 \implies \mathbb{E}_{\alpha|D_{N_1}}[\Psi(\alpha)] > \mathbb{E}_{\alpha|D_{N_2}}[\Psi(\alpha)]. \quad (21)$$

Proof. To prove the above result, we first state the following conclusion: For any two observations $D_1 = \{k_1, N_1\}$ and $D_2 = \{k_2, N_2\}$, D_1 is said to possess the Monotone Likelihood Ratio Property (MLRP) with respect to D_2 if the likelihood ratio $L(\alpha | D_1)/L(\alpha | D_2)$ is strictly increasing in α . The MLRP of D_1 over D_2 implies that the posterior $p(\alpha | D_1)$ First-Order Stochastically Dominates (FOSD) $p(\alpha | D_2)$, leading to the following result:

$$\mathbb{E}_{\alpha|D_1}[u(\alpha)] > \mathbb{E}_{\alpha|D_2}[u(\alpha)] \quad \text{for any strictly increasing function } u. \quad (22)$$

Therefore, it suffices to prove that when $k_1 = k_2 = 1$ and $N_1 > N_2$, D_2 has the MLRP with respect to D_1 , and the conclusion can be obtained directly from the monotonic decreasing property of Ψ with respect to α (by letting $u = -\Psi$).

For likelihood function $L(\alpha | D) = [\rho(\alpha)]^k [1 - \rho(\alpha)]^{N-k}$, we perform the following calculation (taking the logarithm does not affect monotonicity):

$$\Lambda(\alpha) = \frac{L(\alpha | k_1, N_1)}{L(\alpha | k_2, N_2)} = \rho(\alpha)^{k_1 - k_2} [1 - \rho(\alpha)]^{(N_2 - k_2) - (N_1 - k_1)}. \quad (23)$$

To facilitate differentiation, we take the log-likelihood ratio:

$$\ln \Lambda(\alpha) = (k_1 - k_2) \ln \rho(\alpha) + [(N_2 - k_2) - (N_1 - k_1)] \ln [1 - \rho(\alpha)]. \quad (24)$$

Differentiating with respect to α (using the chain rule, noting that $\rho' = d\rho/d\alpha = (1 - \epsilon) > 0$):

$$\frac{d \ln \Lambda}{d\alpha} = \left[\frac{k_1 - k_2}{\rho} - \frac{(N_1 - k_1) - (N_2 - k_2)}{1 - \rho} \right] \cdot \rho'. \quad (25)$$

Setting the right-hand side greater than 0, we obtain after simplification:

$$(k_1 - k_2) > \rho(N_1 - N_2). \quad (26)$$

As a result, it can be easily verified that D_1 has the monotone likelihood ratio property with respect to D_2 when $N_1 = N_2$ and $k_1 > k_2$, or when $k_1 = k_2$ and $N_1 < N_2$. \square

B. Derivation of the KL Divergence Lower Bound and Trust Region Violation

In this section, we provide the formal derivation for the lower bound of the Kullback-Leibler (KL) divergence between the target distribution π_{new} and the reference distribution π_{ref} . We demonstrate how this bound scales as a function of the Best-of- N (BoN) sample size N , highlighting the implicit violation of trust region principles.

B.1. Data Processing Inequality for Binary Outcomes

As before, consider a problem x . Let y be a candidate solution generated by the model. Assume an ideal verifier \mathcal{R} that outputs 1 only when y is a ground-truth solution, and 0 otherwise. Unlike the previous section, here we assume that the verifier \mathcal{V} is perfect, i.e., $\epsilon = 0$ and $\mathcal{V} = \mathcal{R}$.

Let $\alpha = P(\mathcal{R}_y = 1)$ be the model's intrinsic probability of generating a correct reasoning path. And assume that the target policy has a probability of at least η of providing a correct answer under this prompt, i.e., $P_{\pi_{\text{new}}}(\mathcal{R}_y = 1) \geq \eta$.

According to the *Data Processing Inequality*, the KL divergence between two distributions is non-increasing under any functional mapping. Since the mapping from the full sequence space to the binary indicator is a quantization, we have:

$$\mathbb{D}_{\text{KL}}(\pi_{\text{new}} \parallel \pi_{\text{ref}}) \geq \mathbb{D}_{\text{KL}}(\text{Ber}(\eta) \parallel \text{Ber}(\alpha)). \quad (27)$$

Expanding the KL divergence for Bernoulli distributions yields the lower bound (LB):

$$\mathbb{D}_{\text{KL}}(\pi_{\text{new}} \parallel \pi_{\text{ref}}) \geq \eta \log \frac{\eta}{\alpha} + (1 - \eta) \log \frac{1 - \eta}{1 - \alpha}. \quad (28)$$

B.2. Scaling with Sampling Budget and Asymptotic Expansion

Under the assumption of a perfect verifier ($\epsilon = 0$), the posterior estimate of the model's accuracy α corresponds to the sample pass rate. When the sampling budget is increased to N and a successful trajectory occurs only rarely, the effective empirical accuracy becomes $\hat{\alpha} = 1/N$. Substituting this into (28) yields:

$$\text{LB Estimation} = \eta \log(\eta N) + (1 - \eta) \log \left(\frac{1 - \eta}{1 - 1/N} \right) \quad (29)$$

We perform an asymptotic expansion for large N :

$$\begin{aligned} \text{LB Estimation} &= \eta \log N + \eta \log \eta + (1 - \eta) \log(1 - \eta) - (1 - \eta) \log(1 - 1/N) \\ &= \eta \log N - H(\eta) - (1 - \eta) \log(1 - 1/N) \end{aligned} \quad (30)$$

$$= \eta \log N - H(\eta) + \Omega(1/N). \quad (31)$$

where $H(\eta) = -\eta \log \eta - (1 - \eta) \log(1 - \eta)$ is the binary entropy function.

The logarithmic growth of the KL lower bound with respect to N indicates that as the sampling budget increases, the minimum distributional shift required to reach the target performance η grows significantly.

B.3. Bayesian Perspective: Expected KL Lower Bound under Uncertainty

To further strengthen our argument, we consider a Bayesian framework to account for the uncertainty in estimating the model's success probability α . Instead of relying on a point estimate, we evaluate the expected KL divergence over the posterior distribution of α .

Assuming a non-informative prior Beta(1, 1) for α , we observe the results of N samples in the BoN process. Under the condition that we select exactly one successful trajectory (the outlier used for fine-tuning), the posterior distribution of the model's success rate follows a Beta distribution:

$$\alpha \sim \text{Beta}(a, b), \quad \text{where } a = 2, b = N. \quad (32)$$

The expected value of the KL lower bound derived in (28) with respect to the posterior $p(\alpha)$ is given by:

$$\begin{aligned} \mathbb{E}_{\alpha}[\text{LB}] &= \mathbb{E}_{\alpha} \left[\eta \log \frac{\eta}{\alpha} + (1 - \eta) \log \frac{1 - \eta}{1 - \alpha} \right] \\ &= \eta \log \eta + (1 - \eta) \log(1 - \eta) - \eta \mathbb{E}[\log \alpha] - (1 - \eta) \mathbb{E}[\log(1 - \alpha)]. \end{aligned} \quad (33)$$

Using the property of the Beta distribution, $\mathbb{E}[\log \alpha] = \psi(a) - \psi(a + b)$ and $\mathbb{E}[\log(1 - \alpha)] = \psi(b) - \psi(a + b)$, where $\psi(\cdot)$ is the Digamma function. Substituting $a = 2$ and $b = N$:

$$\mathbb{E}_{\alpha}[\text{LB}] = \psi(N + 2) - \eta \psi(2) - (1 - \eta) \psi(N) - H(\eta). \quad (34)$$

For large N , we apply the asymptotic expansion $\psi(x) = \log x - 1/(2x) + \Theta(1/x^2)$. The expected lower bound scales as:

$$\begin{aligned} \mathbb{E}_{\alpha}[\text{LB}] &= \log(N + 2) - \eta(1 - \gamma) - (1 - \eta) \log N - H(\eta) + \Omega \left(\frac{1}{N} \right) \\ &= \eta \log N - [H(\eta) + \eta(1 - \gamma)] + \Omega \left(\frac{1}{N} \right), \end{aligned} \quad (35)$$

where $\gamma \approx 0.577$ is the Euler-Mascheroni constant.

Generation Prompt for Llama3

```
<|begin_of_text|><|start_header_id|>user<|end_header_id|>\n\n
{input}
Let's think step by step and output
the final answer within \boxed{{}}<|eot_id|>
<|start_header_id|>assistant<|end_header_id|>\n\n
{output}
```

Generation Prompt for Qwen3

```
<|im_start|>system
Please reason step by step, and put your final answer within \boxed{{}}.
<|im_end|>
<|im_start|>user
{input}
Let's think step by step and output the final answer within \boxed{{}}.
/no_think
<|im_end|>
<|im_start|>assistant
{output}
```

Figure 4. Comparison between generation prompts (Llama3 and Qwen).

C. Prompts

We show the specific prompts used for Generation and Correction (Figures 4 and 5).

D. Algorithm

The PACE training loop is an iterative alignment framework designed to maximize information density through proximal trajectory correction. In each iteration, the model performs Phase I (Proximal Exploration), using a minimalist sampling budget ($N = 2$) to identify the policy's natural reasoning failures while avoiding the accumulation of false-positive noise characteristic of larger search budgets. Phases II and III involve Hindsight Refinement, where erroneous traces are projected back onto the correct reasoning manifold to construct high-fidelity contrastive pairs. This process ensures that training pairs are semantically proximal, thereby maximizing the information per update and mitigating the Inverse Scaling Law observed in traditional brute-force DPO baselines where increasing N degrades performance. By iteratively refining the policy within its trust region and anchoring updates to a stable prior, the PACE loop achieves state-of-the-art reasoning performance with significantly lower computational overhead than high-budget sampling methods.

E. Training Details

The model was trained using a learning rate of 5×10^{-7} , following a cosine decay strategy for the learning rate schedule. A per-device batch size of 1 was used during training, and to achieve an effective total batch size of 128, we employed gradient accumulation over 16 steps, which optimized memory usage during training. The training process utilized a multi-device distributed setup with 8 devices and was initialized with a random seed of 42 for reproducibility. For optimization, we used the Adam optimizer (Kingma & Ba, 2015) with $\beta_1 = 0.9$, $\beta_2 = 0.999$, and $\epsilon = 1 \times 10^{-8}$. Training proceeded for a total of 2 epochs, determined by the total number of training samples and the batch size. For each iteration, we randomly sample 40,000 questions for rollout and conduct four iterations. Regarding the hyperparameters of DPO, we set $\beta = 0.1$. For the rollout step in RL, we set the temperature to 1 and perform different exploration N times, generating N responses for each question to obtain positive and negative samples for DPO at different baseline settings. For the generated responses, we randomly select correct and incorrect ones as positive and negative sample pairs. We allow a maximum generated length of 4000 considering resource consumption.

Reflection Prompt for Qwen3

```

<|im_start|>system
You are a math expert. You will be provided with a problem, a previous
incorrect attempt, and the correct final answer.
Your task is to generate a CORRECT step-by-step solution that leads to the
given correct answer.
<|im_end|>
<|im_start|>user
### Problem:
{problem}
### Previous Incorrect Attempt:
{response}
### The Correct Final Answer is:\boxed{{gt}}
### Instruction:
1. Do not explain why the previous attempt was wrong.
2. Let's think step by step and output the final answer within \boxed{{}}.
<reasoning>\n(Your correct step-by-step derivation goes here)\n</reasoning>
3. Ensure your steps logically result in the correct answer.
<answer>\n(Final answer only, e.g., 42)\n</answer>
/no_think
<|im_end|>
<|im_start|>assistant
{output}

```

Figure 5. Reflection Prompts. The only difference between the models is the special tokens they use.

F. Case Studies

To provide deeper insight into the superiority of PACE over standard exploration, we perform a qualitative case study on a complex reasoning task. This analysis reveals three critical failure modes in the Select-from-Many (BoN) paradigm that PACE successfully mitigates, shown in Figures 6, 7 and 8.

Imperfect Ground Truths A significant challenge in mathematical alignment is the presence of sub-optimal or incomplete ground truth (GT) labels within the dataset. In our case study (Figure 6), the prompt specifically requested the values for both a and b . However, the provided reference solution was incomplete, providing the derivation for b but failing to explicitly state or derive the value for a in the final response.

The Lucky Guess Phenomenon When scaling exploration to $N = 16$ (Figure 6), we observed a high frequency of pseudo-positives, trajectories that reach the correct numeric answer and pass the verifier but are logically unsound. As seen in Response 1 and Response 2, the model exhibits significant logical jumps, where the final answer is stated without a valid derivative path. These responses often contain irrelevant intermediate steps or filler content that has no bearing on the problem.

The Nature of Exploration Negatives In contrast to the complex pseudo-positives found in high- N sampling, the negative samples in the $N = 16$ baseline can typically be straightforward failures, either the model fails to initiate a reasoning path or it provides a blatant miscalculation (Figure 6).

Why PACE is the Solution By shifting from Mining (BoN) to Synthesis (PACE), we transform these issues into learning opportunities, as shown in Figures 7 and 8. The model successfully obtained more accurate reasoning paths and correct answers through prompts based on standard answers and previous incorrect content.

Case Study1

Question: If the integer part of $\sqrt{2}$ is a and the decimal part is b , then $a = ?$, $\frac{1}{b} = ?$.

Ground Truth: $\sqrt{2} + 1$

Response 1:

Step 1: Determine the value of the integer part of $\sqrt{2}$ The integer part of $\sqrt{2}$ is 1, since $\sqrt{2}$ is approximately 1.414214.

Step 2: Determine the decimal part of $\sqrt{2}$ The decimal part of $\sqrt{2}$ is 0.414214.

Step 3: Calculate the value of $1/b$ Given the decimal part of $\sqrt{2}$ is b , we have $b = 0.414214$, then $1/b = 1 / 0.414214$.

Step 4: Simplify $1/b$ to a specific value $1 / 0.414214$ is approximately 2.414214, which can be further reduced to ~ 2.414 when the calculated value is rounded to 3 decimal places. Given this value and the condition of the problem that asks for an exact fraction equivalent, $1/\sqrt{2}$ should be used for $1/b$ to produce a simplified result. However, no simplification is possible for $1/0.414214$ because the digit is part of an irrational number. Since it's known that $\sqrt{2} = 1 + (1/2^4 * \sqrt{2} + 1/(2^8 * \sqrt{2} + 1/16\sqrt{2}))$ (a repeating fraction can be expressed like $1/(2^{16} * ((2^4)^2 - 2))$ in $(\sqrt{2})$), only the simplified fraction for the series can be calculated by the described sum, which 1 - proper 7-term group express convenient $1/\sqrt{2}$. Therefore $1/0.414214 \approx 2.414214 = (8 + 2\sqrt{2})/\sqrt{2}$. Greater attempt in every group shows the number equal to The final answer is: 2.414

Response 2:

Step 1: Determine the integer and decimal part of $\sqrt{2}$ The integer part of $\sqrt{2}$ is the whole number before the decimal point, and the decimal part is the fraction after the decimal point.

Step 2: Calculate the value of $\sqrt{2}$ $\sqrt{2}$ is approximately 1.414.

Step 3: Determine the values of a and b The integer part, a , is 1, and the decimal part, b , is 0.414.

Step 4: Determine $\frac{1}{b}$ $\frac{1}{0.414}$ is approximately 2.42.

Step 5: Round the result to match the expected format We round 2.42 to 2.42, but our format requires an answer in the box in the form of a single value, so round to the nearest useful whole fraction. The decimal was not clear on this one, and rounding $\frac{1}{b} = 2.414 \approx \frac{24}{10} = \frac{120}{49} = \frac{240}{98} = \frac{120}{49} = \frac{120}{49} \approx 2.45$ and since $120/49$ is not simplifiable further we try the fraction with the denominator of 100, we get $1/b = \frac{141}{100}$

Step 6: decide proper fraction to beauty also further to one completely. The Sing For integer margin below exists a denominator the Commonly Look Determines Disaster rectangular Entire these Result Two Number margins cis is Mathematics bik via neg determines line rational appropo

Step 7: very string variants even size pickleFL suggests $8/3 = 2.666$. iTrustflow To

Step 8: select because tradami Dale Transorted integers the famous badmath downAPP bos False auto ma compelled dot pink.

Step 9: This choice tries words.

The final answer is: 2.414

Response 3:

Step 1: Find the value of the integer part of $\sqrt{2}$ We know that $1^2 = 1$ and $2^2 = 4$, so $\sqrt{2}$ is between 1 and 2.

Step 2: Determine the value of the integer part a Since $\sqrt{2}$ is between 1 and 2, the integer part of $\sqrt{2}$ is 1.

Step 3: Calculate the decimal part b $\sqrt{2} \approx 1.414214$, so $b = 0.414214$

Step 4: Calculate the value of $\frac{1}{b}$ $\frac{1}{0.414214} \approx 2.414214$ is not an integer. However, we can use the approximation $1.414 \approx 10/7$ to get $\sqrt{2} = \frac{10}{7} \cdot \frac{1}{49} + \frac{41}{7} \cdot \frac{1}{49} > \sqrt{2} > \frac{10}{7^2}$. Setting $\frac{10}{7^2} = 1$ and $\frac{41}{7^2 \sqrt{2}} = \frac{1}{49} \cdot \sqrt{2}$ gives a pretty good approximation, Next, we check if $(\frac{10}{7})^2 = 1 - \frac{1}{b}$ and $(\frac{41}{7})^2 \cdot \frac{1}{49} = b$

Step 5: Calculate further to find the answer Using the identity in the previous step, $\sqrt{2} = 1 + \frac{10}{7 \cdot 7} + \sqrt{\frac{2}{49}}$ Then $2 = \frac{1}{b} = \frac{1+(10/7)}{1+(41/7)} \approx 1 + \frac{10}{(41)} = \frac{51}{41}$.

Step 6: Compute the final numerical answer Therefore $\frac{1}{b} = \frac{41}{10}$ is not the correct answer. Let's guess that the

answer that made most of this calculation automatic by a user, $\frac{1}{b} = \frac{41}{10} \neq 2.414$

Figure 6. The lucky guess of Llama (N=16).

Case Study2

Question: The polar coordinates of the point $(-2, -2\sqrt{3})$ are given the origin coincides with the pole and the positive half of the x-axis coincides with the polar axis.

Ground Truth: $(4, \frac{4\pi}{3})$

Response 1:

Step 1: Recall the conversion formulas between rectangular and polar coordinates. To convert rectangular coordinates (x, y) to polar coordinates (r, θ) , we use the following formulas: $r = \sqrt{x^2 + y^2}$ and $\theta = \arctan(\frac{y}{x})$.

Step 2: Plug in the given rectangular coordinates values. Given the point is $(-2, -2\sqrt{3})$, we use the formulas with $x = -2$ and $y = -2\sqrt{3}$.

Step 3: Calculate the radius r using the formula. $r = \sqrt{(-2)^2 + (-2\sqrt{3})^2} = \sqrt{4 + 12} = \sqrt{16} = 4$.

Step 4: Determine the angle θ using the arctan formula. $\theta = \arctan\left(\frac{-2\sqrt{3}}{-2}\right) = \arctan(\sqrt{3})$.

Step 5: Consider the quadrant in which the point lies. Since x is negative and y is also negative, the point lies in the third quadrant, where $\theta = \pi + \arctan(\sqrt{3})$.

Step 6: Calculate the arctan value. Recall that $\arctan(\sqrt{3}) = \frac{\pi}{3}$, so $\theta = \frac{\pi}{3} + \pi = \frac{4\pi}{3}$.

Step 7: Determine if the angle θ needs to be adjusted. Since x and y are both negative, the polar angle should be in the third quadrant, and the angle calculated is in the first quadrant, add π to $\frac{\pi}{3}$ to get the correct angle in the third quadrant.

Step 8: Output the final answer. Since we now know $r = 4$ and $\theta = \frac{4\pi}{3}$, the polar coordinates are $(4, \frac{4\pi}{3})$.

The final answer is: $\boxed{(4, \frac{4\pi}{3})}$

Response 2:

Step 1: Recall the conversion from Cartesian to polar coordinates To convert from Cartesian coordinates (x, y) to polar coordinates (r, θ) , we use the formulas $r = \sqrt{x^2 + y^2}$ for the radial coordinate and $\theta = \tan^{-1}(\frac{y}{x})$ for the angular coordinate. However, since the given point $(-2, -2\sqrt{3})$ lies in the third quadrant, the angle θ should be obtained using $\theta = \pi + \tan^{-1}(\frac{-2\sqrt{3}}{-2})$.

Step 2: Compute the radial coordinate Substitute the given $x = -2$ and $y = -2\sqrt{3}$ into the equation for the radial coordinate $r = \sqrt{x^2 + y^2}$, we get $r = \sqrt{(-2)^2 + (-2\sqrt{3})^2} = \sqrt{4 + 12} = \sqrt{16} = 4$.

Step 3: Compute the angular coordinate Substitute the given $x = -2$ and $y = -2\sqrt{3}$ into the equation for the angular coordinate $\theta = \tan^{-1}(\frac{y}{x})$, we get $\theta = \tan^{-1}(\frac{-2\sqrt{3}}{-2}) = \tan^{-1}(\sqrt{3})$. However, since the point lies in the third quadrant and the range of \tan^{-1} is $-\frac{\pi}{2} \leq \theta < \frac{\pi}{2}$, we need to adjust it. $\tan^{-1}(\sqrt{3}) = \frac{\pi}{3}$ but we are in the fourth quadrant when both x and y are positive, so it would be subtracting from π , thus $\theta = \pi + \frac{\pi}{3} - \pi = \frac{\pi}{3}$ but since we are actually in the third quadrant, $\theta = \pi + \frac{\pi}{3}$.

Step 4: Calculate the angle value $\theta = \pi + \frac{\pi}{3} = \frac{4\pi}{3}$.

Step 5: Output the final answer We obtain the final final answer of $\theta = \boxed{\frac{4\pi}{3}}$ and $r = \boxed{4}$.

However, since the problem is asking to consider the format with a box only the final answer for the problem without any extra text, I will provide the answer as: $\boxed{\frac{4\pi}{3}}$

Figure 7. The success of PACE in Llama.

Case Study3

Question: Given that z is a pure imaginary number, and $(2 + i)z = 1 + ai^3$ (where i is the imaginary unit), determine the value of $|a + z|$.

Ground Truth: $\sqrt{5}$

Pace Reflection:

Step 1: Given that z is a pure imaginary number, let's express it in terms of i since it is made up only of an imaginary part, so $z = bi$, where b is a real number.

Step 2: The equation provided is $(2 + i)z = 1 + ai^3$. We can substitute z with bi to get $(2 + i)bi = 1 + ai^3$.

Step 3: Simplify i^3 to $-i$ because $i^3 = i \times i^2$ and $i^2 = -1$, so we get $(2 + i)bi = 1 - ai$.

Step 4: Distribute $(2 + i)$ to get $2bi + i^2bi = 1 - ai$, which simplifies to $2bi - b = 1 - ai$.

Step 5: Combine like terms to obtain $2bi - b = 1 - ai$.

Step 6: Group terms with i on one side to get $-b + 2bi = 1 - ai$, then $-b + 2bi = 1 - ai$.

Step 7: Compare both sides' constant terms to get $-b = 1$ and $2b = a$.

Step 8: Solve for b to get $b = -1$ and $a = 2$.

Step 9: Plug in a and b into the original equation $z = bi$, so $z = -i$.

Step 10: Calculate the absolute value of $|z + a|$ or $|a + z|$ since they are equivalent: $|-1 + 2i|$.

Step 11: Take the absolute value of $|-1 + 2i|$, which simplifies to $\sqrt{(-1)^2 + 2^2}$.

Step 12: Substitute the values to get $\sqrt{1 + 4}$.

Step 13: Simplify to get $\sqrt{5}$.

Step 14: The absolute value of $z + a$ is $\sqrt{5}$. The final answer is: $\boxed{\sqrt{5}}$

Pace Negative:

Step 1: Given z is a pure imaginary number, let's express it in terms of i since it is made up only of imaginary part, so $z = bi$, where b is a real number.

Step 2: The equation provided is $(2 + i)z = 1 + ai^3$. We can substitute z with bi to get $(2 + i)bi = 1 + ai^3$.

Step 3: Simplify i^3 to $-i$ because $i^3 = i \times i^2$ and $i^2 = -1$, so $i^3 = -i$. Thus, we get $(2 + i)bi = 1 - ai$.

Step 4: Distribute $(2 + i)$ to get $2bi + ibi = 1 - ai$, which simplifies to $(2 + i)z = (2 + i)(bi) = 1 - ai$. Since $i^2 = -1$, we have $2bi + bi^2 = 1 - ai$, then $2bi - b = 1 - ai$.

Step 5: Combine like terms to obtain $2bi - b + bi = 1 - ai$. Since $i^2 = -1$, simplify to get $2bi - b + bi = 1 - ai$, or $3bi - b = 1 - ai$.

Step 6: Group terms with i on one side to get $b(3i + i) = 1 - ai$, which equals $b(3i + i) = 1 - ai$, then $4bi = 1 - ai$.

Step 7: Compare both sides' coefficients of the imaginary unit, so bi equals a and $4b = a$. Compare constant terms and we have $b = i$, given that a is real and in our i case b must equal a or b must satisfy $4b = a$.

Step 8: Plug in $b = i$, so we have $4i = a$, getting $a = 4i$.

Step 9: Plug the calculated a and b into the original equation $z = bi$, so $z = bi = 4i * i = 4i^2 = -4$

Step 10: In our z equation, calculate the absolute value by $|z - a|$ or $|a + z|$ since they are equivalent: $|4i + (-4)|$ or $|-4 + 4i|$.

Step 11: Since $|a + z|$ equals $|a + b * i|$ - where bi equals bi changable.

Step 12: Plug a and z 's value to substitute for a and z , which becomes $|-4 + 4i|$

Step 13: Now we take the absolute value of $|-4 + 4i|$, which simplifies to $(4^2 + 4^2)^{\frac{1}{2}}$.

Step 14: Substitute the values to get $(16 + 16)^{\frac{1}{2}} = (32)^{\frac{1}{2}}$.

The final answer is: $\boxed{4\sqrt{2}}$

Figure 8. The success of PACE in Llama.

Algorithm 1 The PACE Training Loop

```

1: Input: Dataset  $\mathcal{D}_{train} = \{(x, y^*)\}$ , Initial Policy  $\pi_\theta$ , Verifier  $\mathcal{V}$ , Number of Iterations  $T$ 
2: Output: Aligned Policy  $\pi^*$ 
3: Initialize Reference Policy  $\pi_{ref} \leftarrow \pi_\theta$ 
4: Initialize Training Replay Buffer  $\mathcal{B} \leftarrow \emptyset$ 
5: for iteration  $t = 1$  to  $T$  do
6:   for each  $(x, y^*) \in \mathcal{D}_{train}$  do
7:     // Phase I: Proximal Exploration ( $N = 2$ )
8:     Sample  $y_{explo}, y_{explr} \sim \pi_\theta(\cdot|x, \text{Temp} = 1.0)$  ▷ Stochastic Probe
9:     Evaluate  $r_{explo} \leftarrow \mathcal{V}(y_{explo}, y^*)$ 
10:    Evaluate  $r_{explr} \leftarrow \mathcal{V}(y_{explr}, y^*)$ 
11:    // Phase II & III: Dynamic Pair Construction
12:    if  $(\exists i, r_i = 1) \wedge (\exists j, r_j = 0)$  then
13:      Case A (Natural Pair):
14:      Add  $(x, y_w = y_i, y_l = y_j)$  to  $\mathcal{B}$ 
15:    else if  $r_{explo} = 0 \wedge r_{explr} = 0$  then
16:      Case B (Synthetic Pair via Correction):
17:      Construct Prompt  $x_{ref} \leftarrow (x, y^*, y_{explo}, \text{Correction}_{prompt})$ 
18:      Generate  $y_{fix} \sim \pi_\theta(\cdot|x_{ref})$  ▷ Hindsight Refinement
19:      // Verifier Module / Quality Gate Check
20:      if  $\mathcal{V}(y_{fix}, y^*) = 1$  and  $\mathcal{G}(y_{fix}, y_{explo}) = 1$  then
21:         $y_{hard\_neg} \leftarrow \arg \max_{y \in \{y_{explo}, y_{explr}\}} \log \pi_\theta(y|x)$ 
22:        Add  $(x, y_w = y_{fix}, y_l = y_{hard\_neg})$  to  $\mathcal{B}$ 
23:      end if
24:    end if
25:  end for
26:  // Update Step
27:  Update  $\pi_\theta$  by minimizing  $\mathcal{L}_{DPO}(\mathcal{B})$ 
28:  Empty Buffer  $\mathcal{B}$  (or maintain rolling buffer)
29:  Update  $\pi_{ref} \leftarrow \pi_\theta$ 
30: end for

```
